

Supplementary Methods

Stimuli, Task and Experimental Protocol

For testing, participants were seated 80 cm (± 10 cm) in front of the stimulus-presentation screen in a dark, sound-attenuated, electrically-shielded recording booth (International Acoustics). A chinrest was provided to minimize head movements. The Spatial CTET was coded with the Presentation software package (Neurobehavioral Systems) and presented on a 26" LCD monitor (ViewSonic model VP2655wb; refresh rate: 60 Hz; resolution: 1680 x 1050 pixels).

Each checkerboard measured 250x250 px (see Figure 1 for visual angle values) and the fixation dot measured 10x10 px. Checkerboard centers were located at 225 px below and 275 px to the left/right of the center of the screen (diagonal distance from screen center to checkerboard center: 355px). Luminance of the background was 25.2 cd/m². For checkerboards, luminance of the lighter gray was 43.3 cd/m²; luminance of the darker grey was 8.3 cd/m².

Targets occurred independently in each checkerboard stream. No information was given to participants about responding to targets in the unattended stream, and no participant reported noticing targets in the unattended stream.

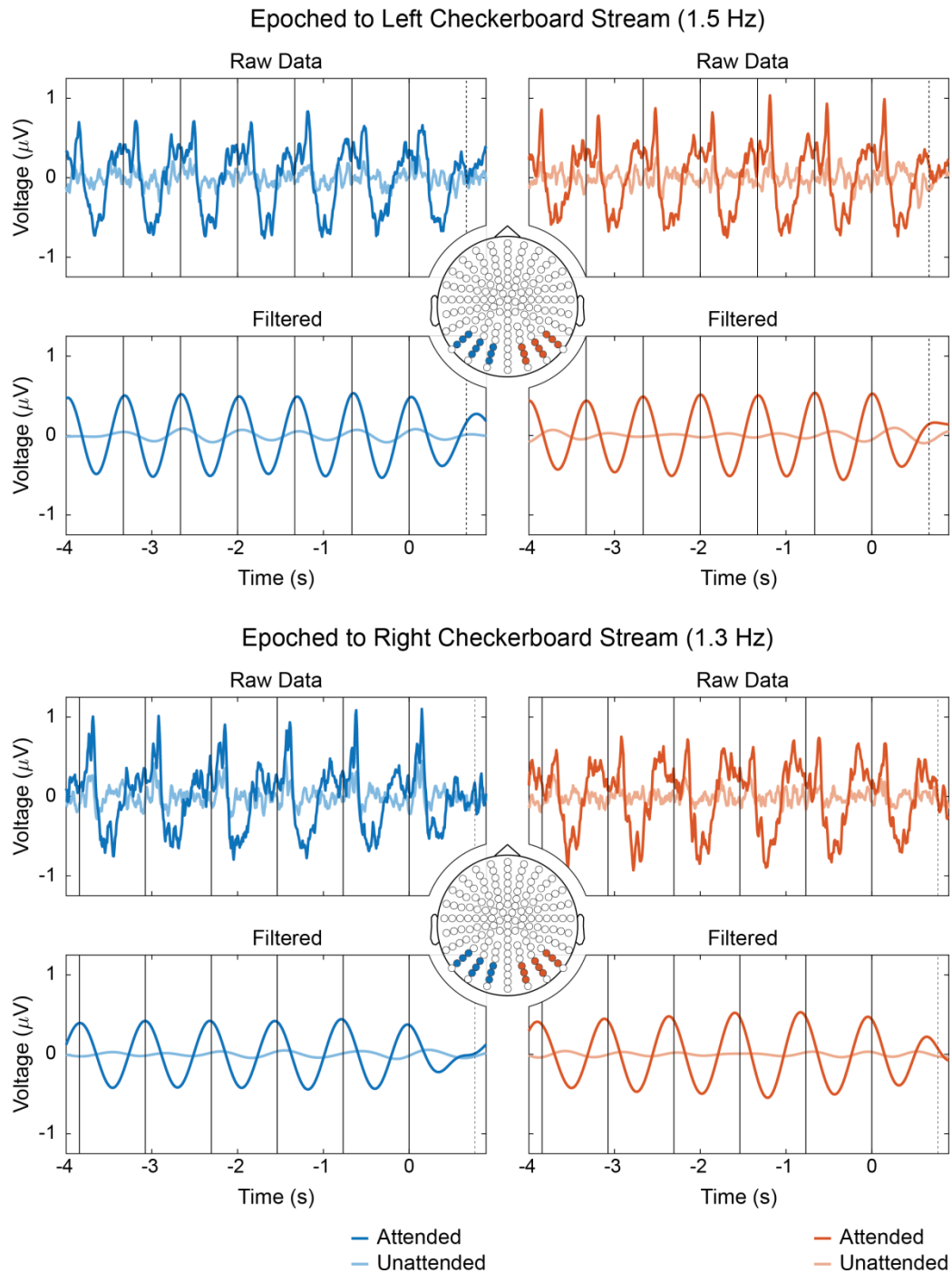
Data Acquisition

In the BioSemi ActiveTwo system, each active electrode integrates the first amplifier stage locally on the electrode, enabling electrode output impedances of less than 1 Ω . Typically the recordings are referenced during acquisition to the active, two-electrode (CMS-DRL; Common Mode Sense-Driven Right Leg) referencing system. In this system, two electrodes (CMS and DRL) near the midline on posterior-parietal scalp are used to create a feedback loop that actively drives the subject's average potential (the Common Mode Voltage) to the reference voltage of the ADC (analog-to-digital converter). As recorded potentials are referenced to the driven CMS electrode and not the potential measured from another recording electrode (or a

group of them), potentials recorded with this referencing system are often labeled “reference-free.” Alternative referencing conventions (any electrode or combination of them) can then be chosen freely offline without loss of information.

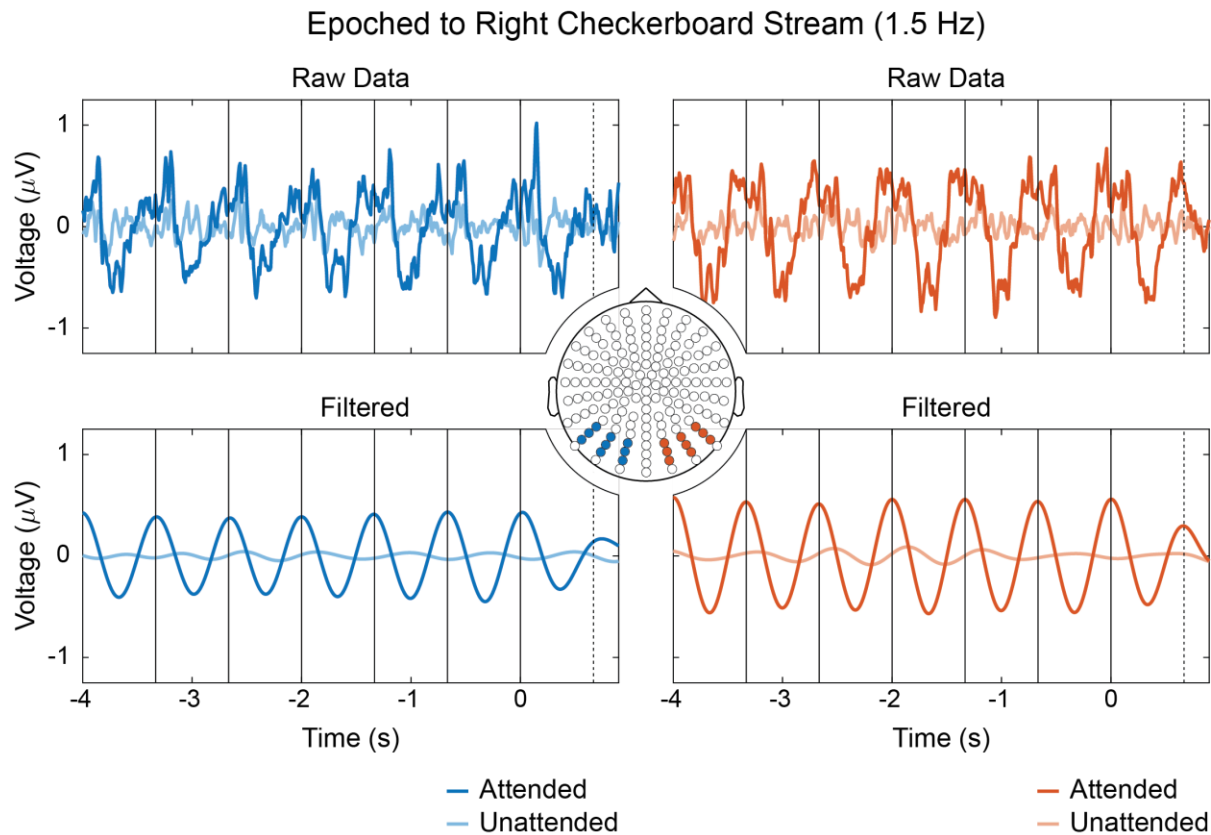
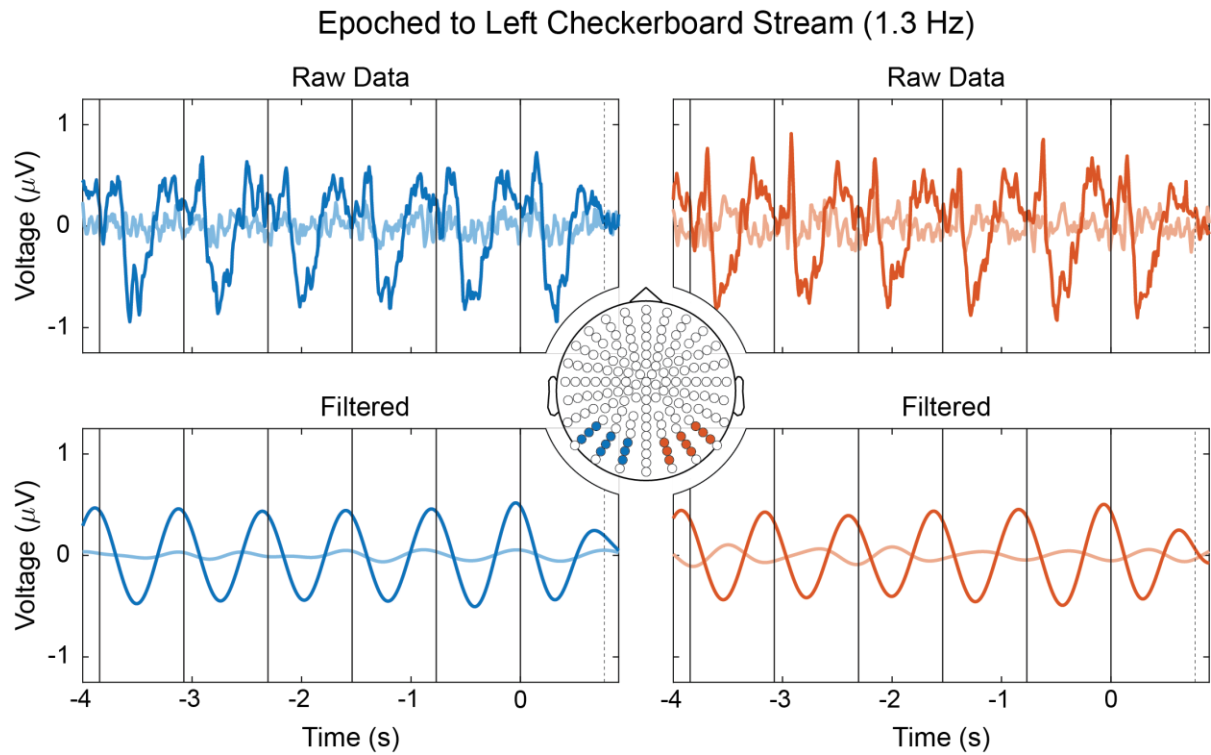
With respect to eye-tracking, the EyeLink 1000 system uses a high-speed camera to capture the infrared light reflected from a subject’s cornea and the darkness of the pupil, enabling calculation of fixation position. In Remote/Head Free mode, fixation measurements have a maximum resolution and accuracy of 0.05° and 0.5° visual angle, respectively.

Supplementary Figures



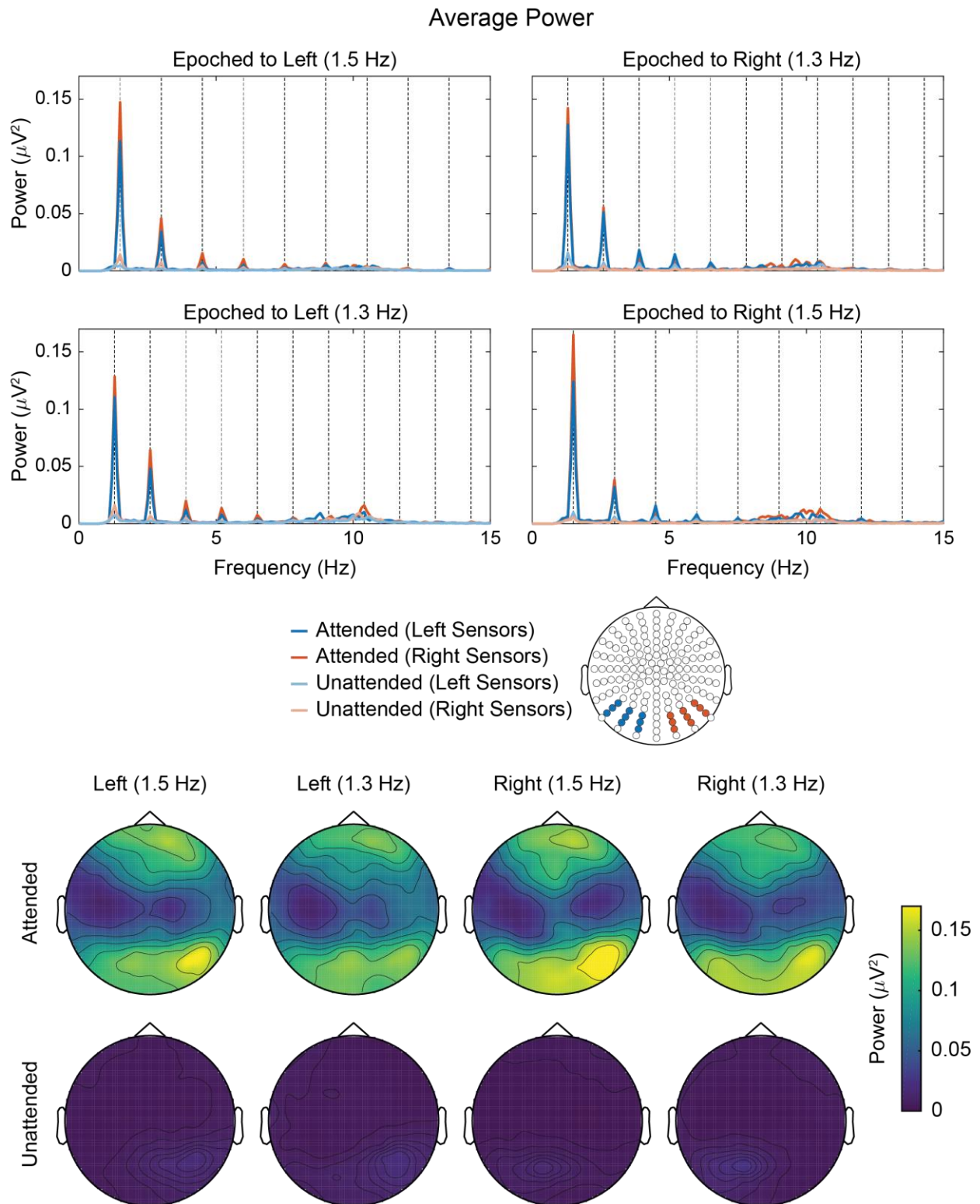
Supplementary Figure 1: Time-locked potentials for the left-fast stimulus configuration. Data epoched to both the left and right checkerboard streams are shown for two posterior sensor groups in the left-fast stimulus configuration (left checkerboard at 1.5 Hz; right at 1.3 Hz). Raw, unfiltered data are shown alongside a delta-filtered (1-2 Hz) equivalent. Attended (hit trials only) and unattended trials are shown. The dashed line indicates the moment at which the next

checkerboard rotation is expected but *does not* occur. The solid black vertical lines indicate actual checkerboard rotations. Unlike Figure 2, the horizontal axis denotes time in seconds instead of checkerboard rotations elapsed.



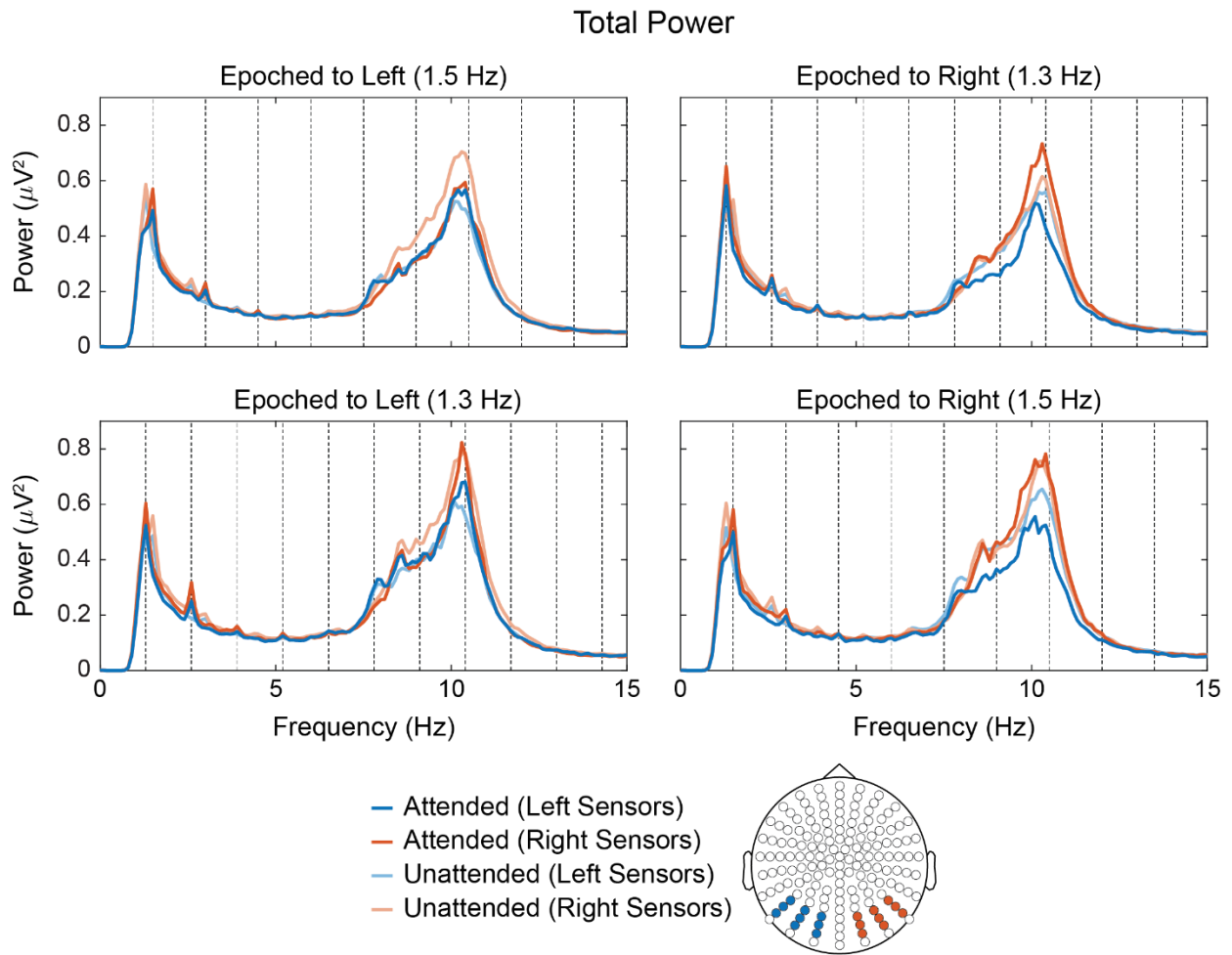
Supplementary Figure 2: Time-locked potentials for the right-fast stimulus configuration. Data epoched to both the left and right checkerboard streams are shown for two posterior sensor

groups in the right-fast stimulus configuration (left checkerboard at 1.3 Hz; right at 1.5 Hz). Raw, unfiltered data are shown alongside a delta-filtered (1-2 Hz) equivalent. Attended (hit trials only) and unattended trials are shown. The dashed line indicates the moment at which the next checkerboard rotation is expected but *does not* occur. The solid black vertical lines indicate actual checkerboard rotations. Unlike Figure 2, the horizontal axis denotes time in seconds instead of checkerboard rotations elapsed.



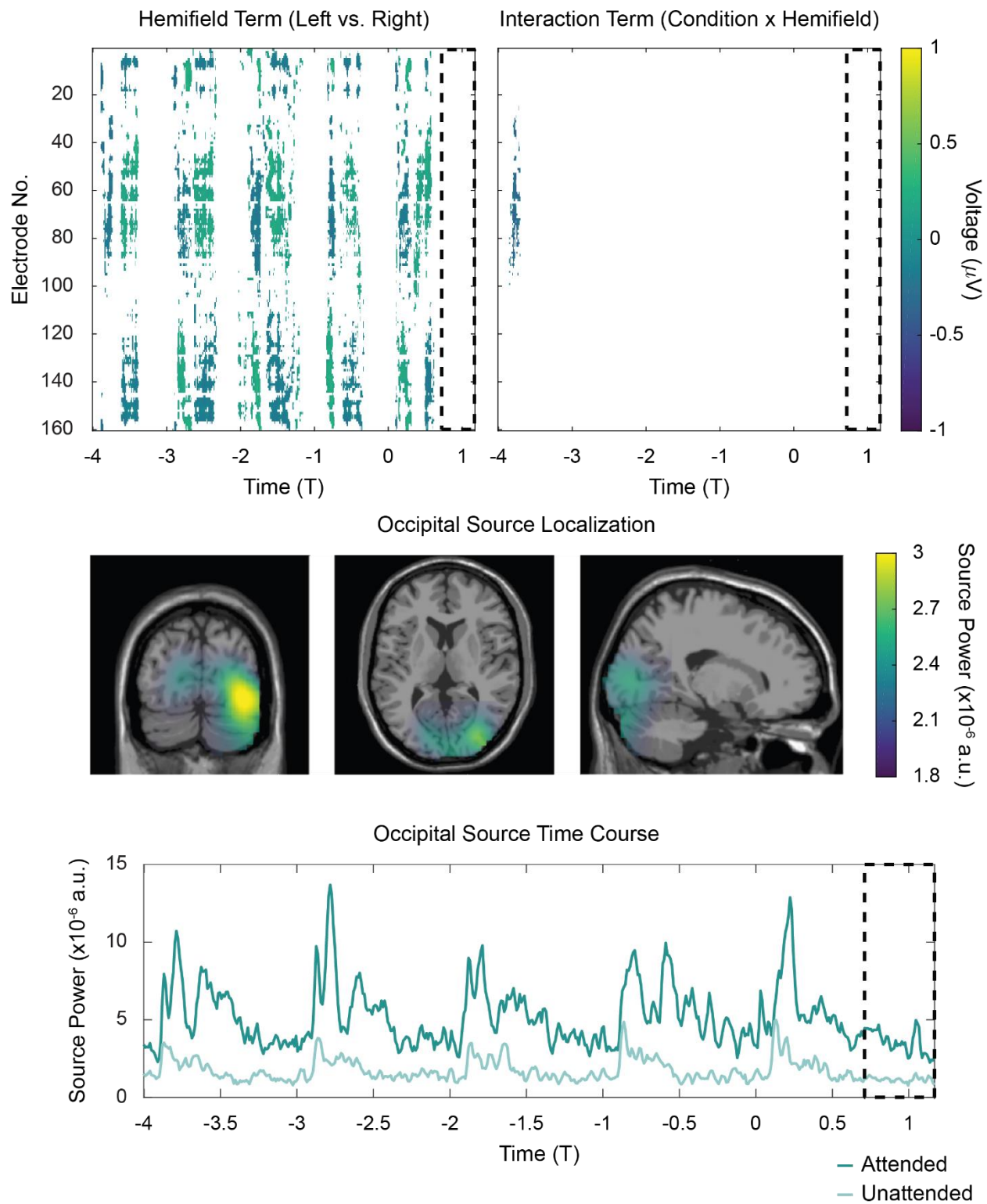
Supplementary Figure 3: Spectral power of averaged data. *Top:* Spectral analysis of the averaged, time-locked data indicates that spectral power is primarily concentrated at the stimulation frequency and its harmonics. Both attended (hit trials only) and unattended conditions are shown, revealing an overall decrease in spectral power at the epoching

frequency during the unattended condition. Dashed vertical lines indicate the epoching checkerboard frequency (1.5 Hz or 1.3 Hz) and its harmonics. *Bottom:* For each condition, spectral power values at the fundamental frequency were extracted for all electrodes and plotted topographically. In addition to an overall decrease in power at the fundamental (as above), unattended topographies also demonstrate a more focal power distribution that is localized primarily to posterior scalp sites contralateral to the epoching checkerboard. In the attended case, however, power at the fundamental is broadly distributed across anterior and (bilateral) posterior scalp sites.



Supplementary Figure 4: Spectral power taken before trial averaging. Spectral power in individual trials was computed via the Fourier transform before averaging power values across trials. Broadband power is evident with peaks at the epoching frequency and its harmonics (dashed vertical lines). A broad peak in the alpha band (8-14 Hz) is also evident. Both attended (hit trials only) and unattended conditions are shown. In the unattended condition, trials were epoching with respect to the unattended checkerboard stream while participants attend the *other* (i.e. attended) checkerboard stream. Therefore, we observe unattended peaks at the non-epoching frequency (e.g. 1.3 Hz for the top left plot). However, this activity (like much of the broadband activity) is not in-phase across trials as demonstrated in Supplementary Figure 3.

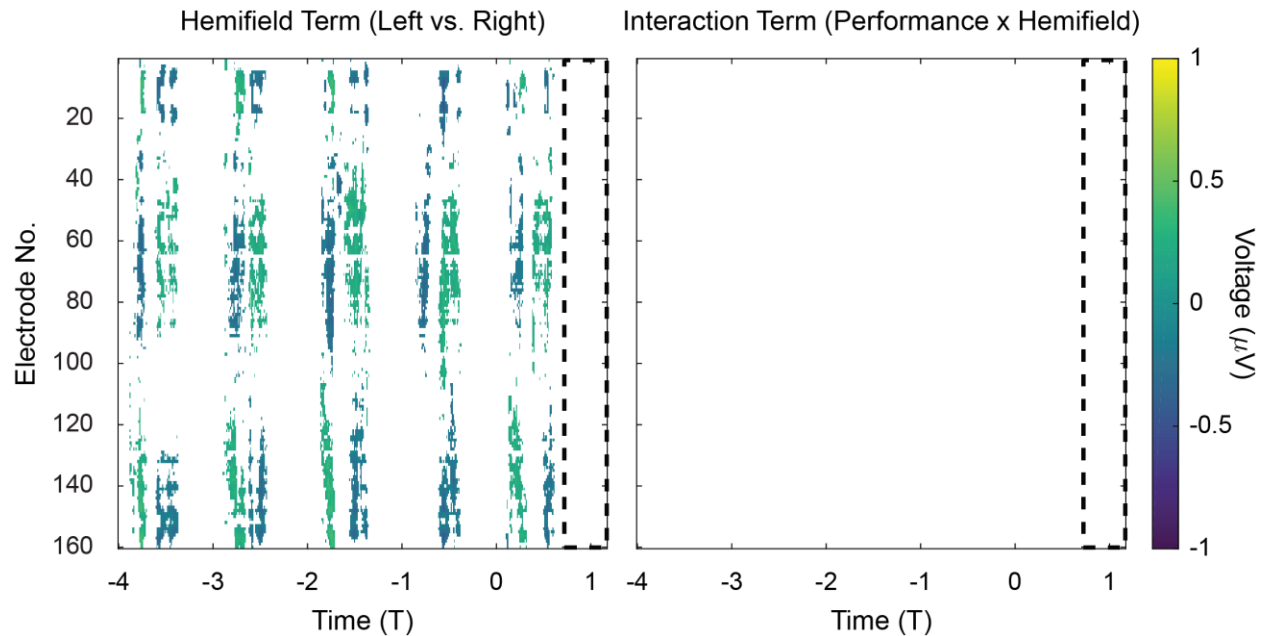
Attention Analysis - Supplemental



Supplementary Figure 5: Supplementary statistical and source analyses on raw data in Figure 2. *Top Left:* Plotted data is the difference between trials epoched to the left checkerboard stream and those epoched to the right checkerboard stream, masked by statistical significance

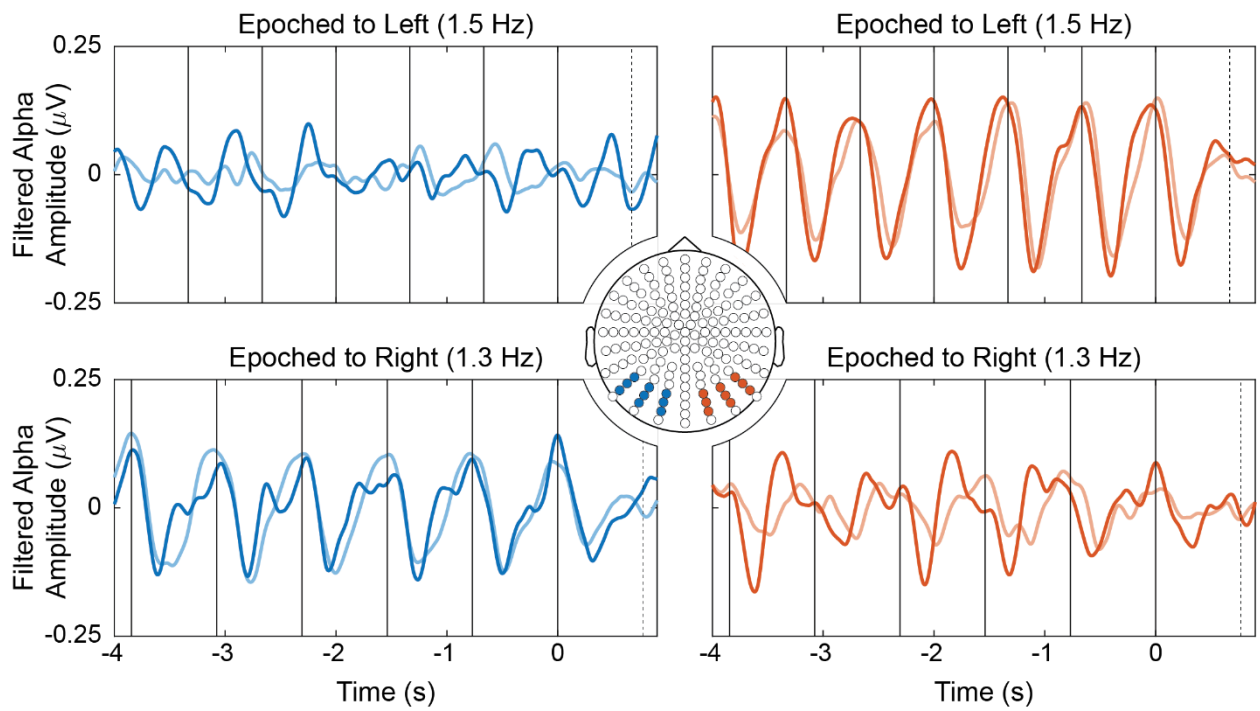
($p < 0.05$) after cluster-corrected permutation testing. *Top Right*: Statistical significance of the interaction term (condition \times hemifield) is plotted and again masked by cluster-corrected statistical significance ($p < 0.05$). For both *Top* plots, the dashed box indicates the time interval surrounding T_1 . *Middle*: Source-localization and masking of anterior regions suggests another (right-lateralized) focal source during the T_1 -interval. *Bottom*: Reconstructed power time-course of the source above. Increased source power is visible after each checkerboard presentation. A small spike is also observed in the T_1 -interval, although we hesitate here to overinterpret its significance.

Performance Analysis - Supplemental Terms

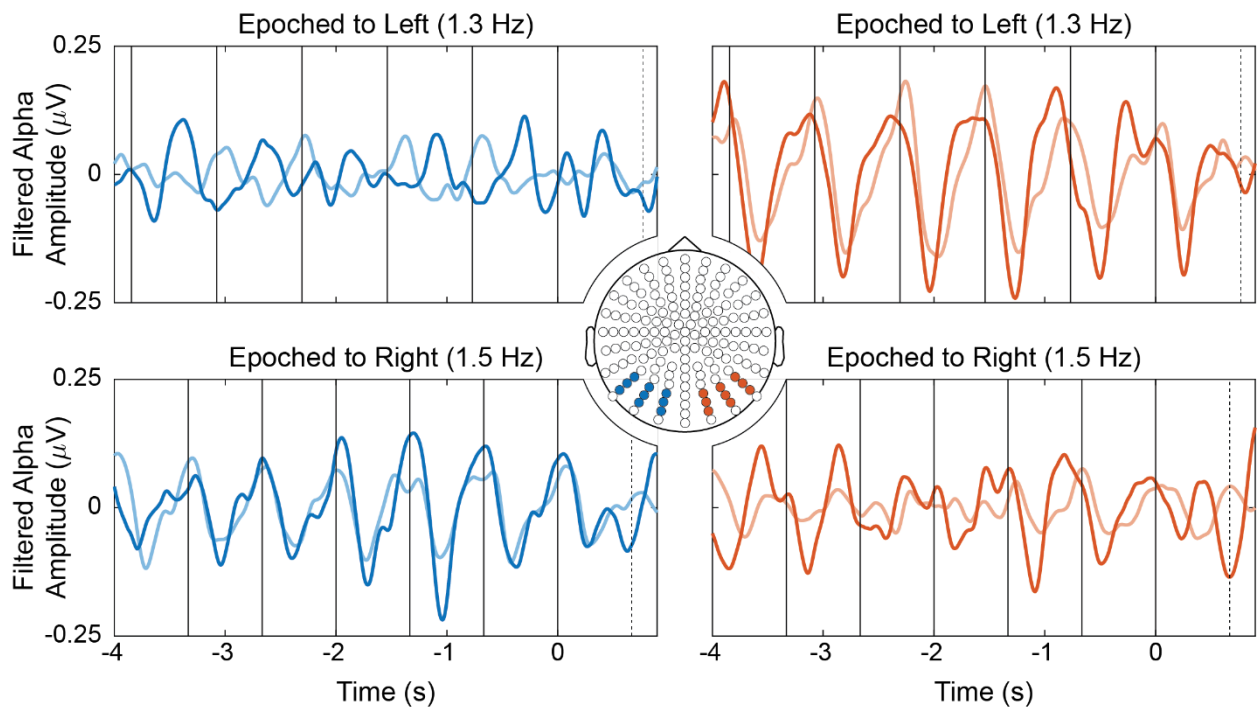


Supplementary Figure 6: Supplementary statistical analysis from raw data in Figure 4. *Left:* Plotted data is the difference between trials epoched to the left checkerboard stream and those epoched to the right checkerboard stream, masked by statistical significance ($p < 0.05$) after cluster-corrected permutation testing. *Right:* Statistical significance of the interaction term (performance x hemifield) is plotted and again masked by cluster-corrected statistical significance ($p < 0.05$). For both *Left* and *Right* plots, the dashed box indicates the time interval surrounding T1.

Left-Fast Stimulus Configuration



Right-Fast Stimulus Configuration

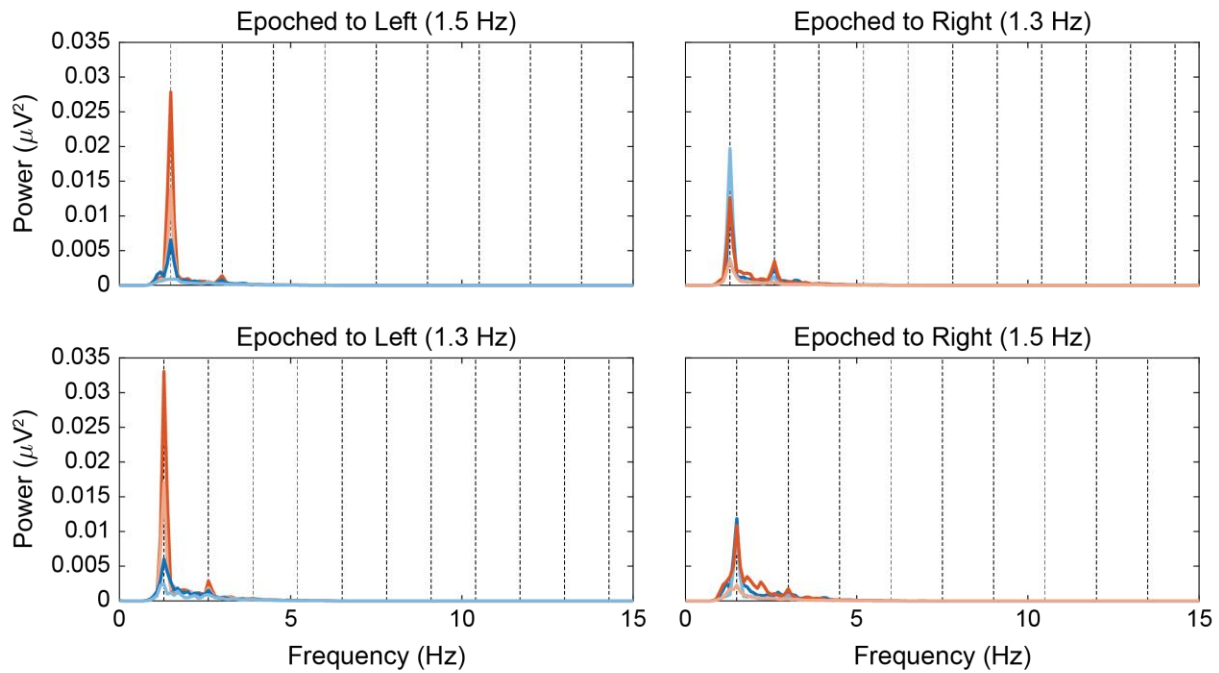


— Attended
— Unattended

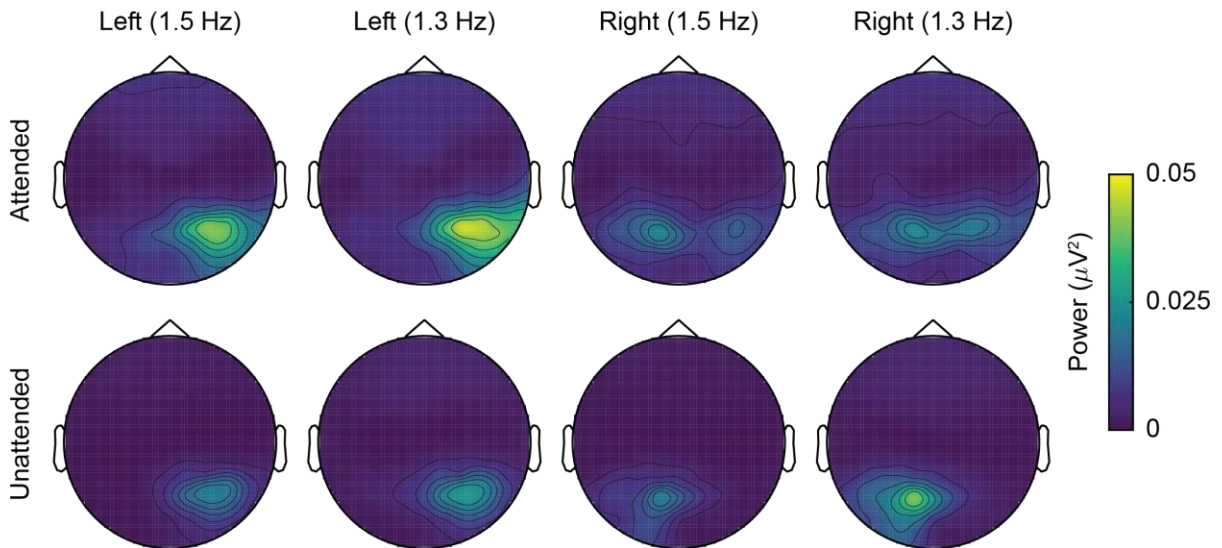
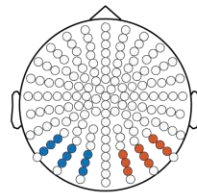
— Attended
— Unattended

Supplementary Figure 7: Time-locked, filtered alpha envelopes. Alpha envelopes were extracted as described in the text. Here, we present the envelopes before conversion to the common time domain and collapse across stimulus configuration for reference. Note that envelopes were high-pass filtered at 1 Hz for baseline correction prior to plotting; negative envelope values therefore indicate deviations in alpha power below the mean (the 0 Hz component) and other low-frequency components. *Top:* Alpha envelopes for the left-fast stimulus configuration, where the left checkerboard rotated at 1.5 Hz and the right rotated at 1.3 Hz. *Bottom:* Alpha envelopes for the right-fast stimulus configuration, where the left checkerboard rotated at 1.3 Hz and the right rotated at 1.5 Hz.

Average Alpha Envelope Power



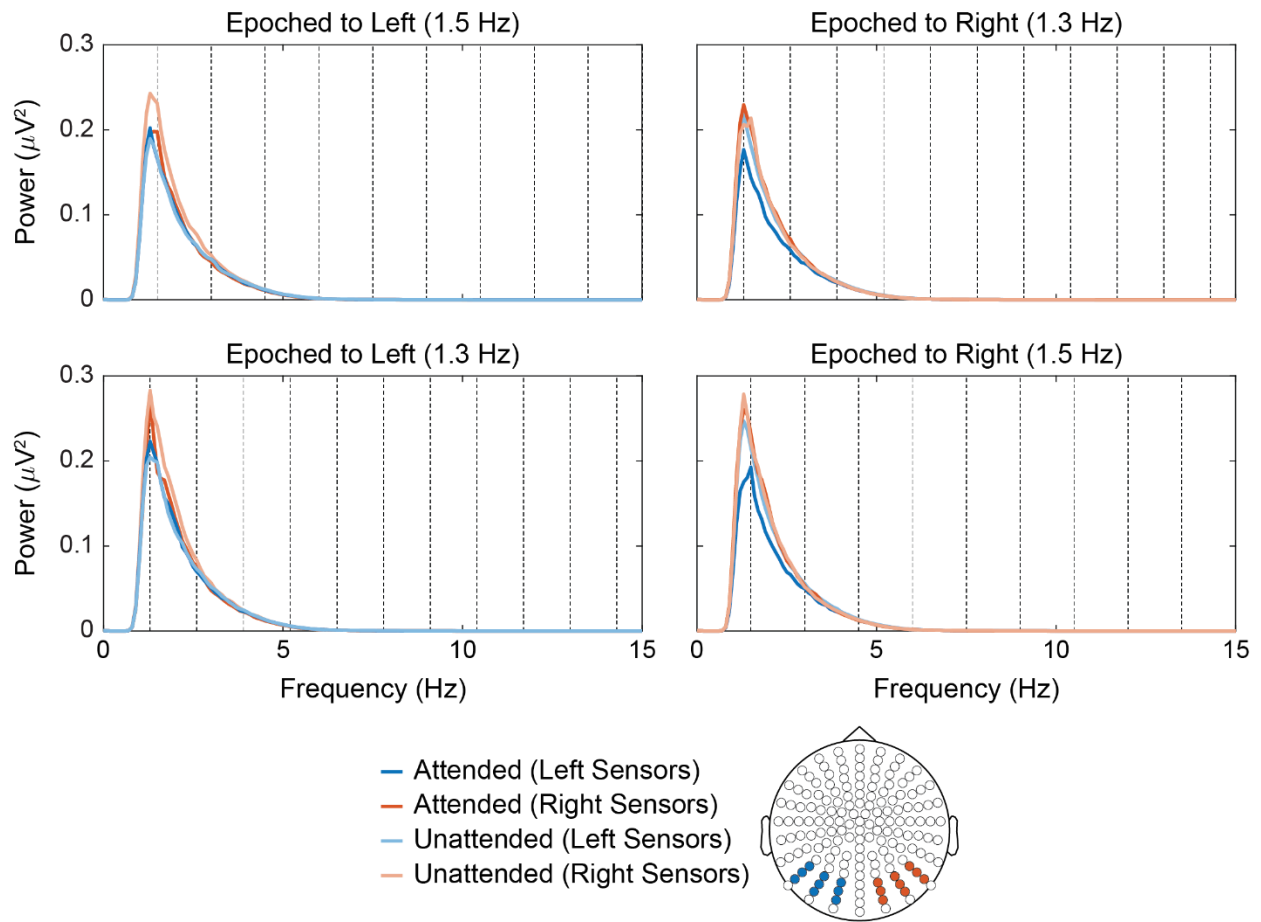
- Attended (Left Sensors)
- Attended (Right Sensors)
- Unattended (Left Sensors)
- Unattended (Right Sensors)



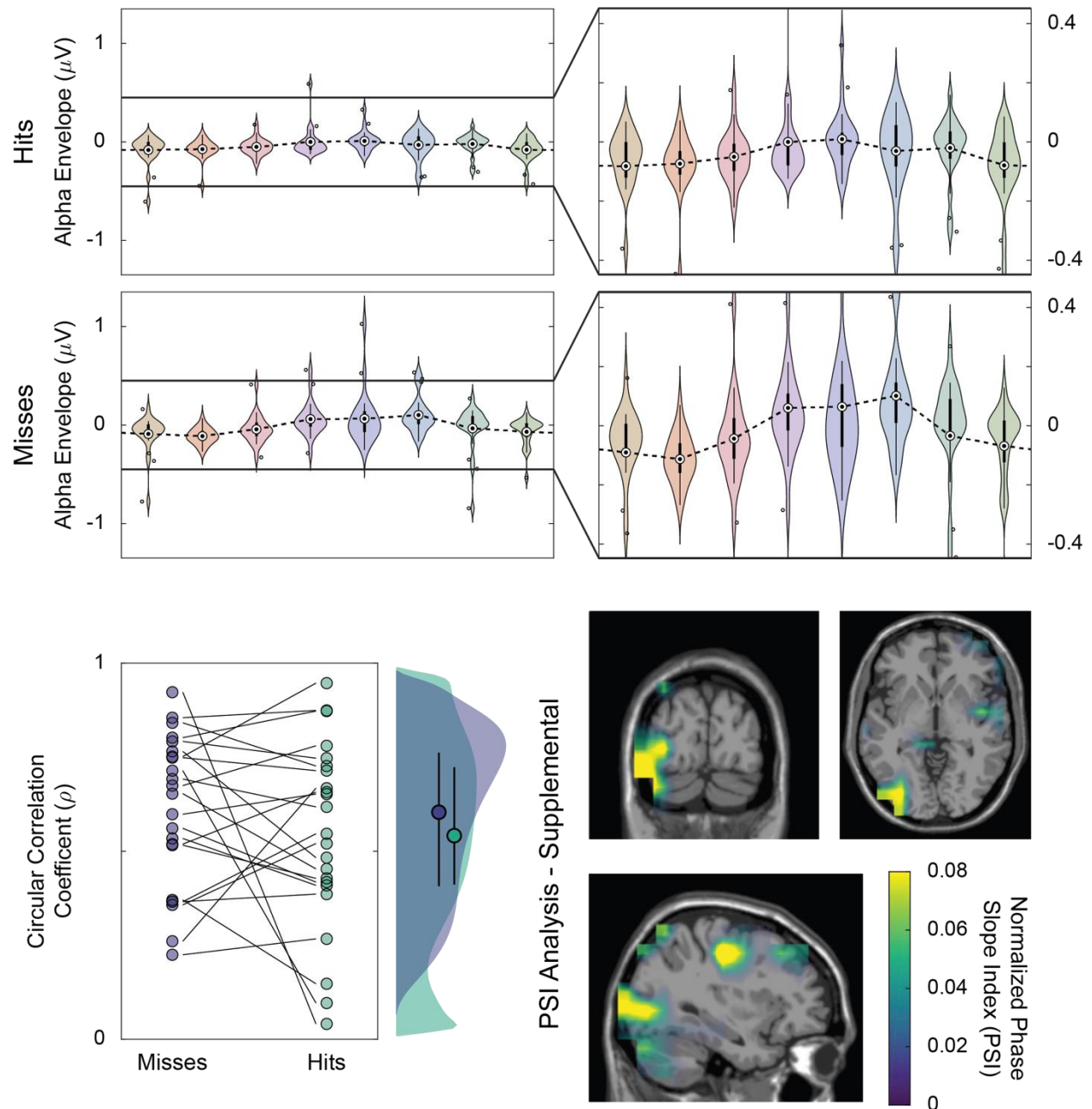
Supplementary Figure 8: Spectral power of averaged alpha envelopes. *Top:* Spectral analysis of the averaged, time-locked envelopes indicates that spectral power is primarily concentrated at the stimulation frequency and its harmonics. Dashed vertical lines indicate the epoching checkerboard frequency (1.5 Hz or 1.3 Hz) and its harmonics. *Bottom:* For each condition,

spectral power values at the fundamental frequency are extracted for all electrodes and plotted topographically for reference.

Total Alpha Envelope Power



Supplementary Figure 9: Spectral power of the alpha envelopes taken before trial averaging. Spectral envelope power in individual trials was computed via the Fourier transform before averaging power values across trials. Dashed vertical lines indicate the epoching checkerboard frequency (1.5 Hz or 1.3 Hz) and its harmonics. Broadband power is evident with occasional peaks at the epoching frequency. Both attended (hit trials only) and unattended conditions are shown.



Supplementary Figure 10: *Top:* Comodulograms show that (high-pass filtered) ipsilateral alpha power is significantly correlated to frontal delta phase. Data is presented in violin plot format as in Figure 5. Zoomed-in violin plots are also shown for convenience. For these analyses, the frontal (blue) sensors in Figure 4, *Top Right* were used to compute frontal delta phase (c.f. Figure 7, where delta phase is estimated from the parietal (green) sensors in Figure 4). Also note: compared to Figure 7, the y-scaling for the non-zoomed (*Top Left*) plots has changed to accommodate the increased variance in the comodulograms. *Bottom Left:* Raincloud plot of individual circular-linear correlation coefficients between the hit and miss conditions. Again, frontal electrodes from Figure 4 are used for delta phase estimation (c.f. Figure 7). Plotting conventions are the same as Figure 7, *Middle Left*. When employing frontal sensors for delta phase estimation, no difference in ρ is observed between hit and miss conditions. *Bottom Right:* PSI analysis performed with a frontal delta seed. Unlike the PSI source-space analysis in Figure

7, *Bottom Right*, PSI analysis was here performed using a mask generated from Figure 3, *Middle* as a seed region. Again, a contrast between the hit and miss conditions is shown. The regions shown above are therefore those voxels whose alpha power is more driven by the entrained frontal delta activity in hits versus misses; again, we find an ipsilateral (left-lateralized after reflection), posterior region where this appears to be the case. We also note the second region visible in the image above, but as we have no mechanistic hypothesis for its relationship to entrained frontal delta activity, we will not comment on it here.